

## Accepted Manuscript

Development of a  $C_3$ -symmetric benzohydroxamate tripod: Trimetallic complexation with Fe(III), Cr(III) and Al(III)

Minati Baral, Amit Gupta, B.K. Kanungo

PII: S1386-1425(16)30090-7  
DOI: doi: [10.1016/j.saa.2016.02.033](https://doi.org/10.1016/j.saa.2016.02.033)  
Reference: SAA 14299

To appear in:

Received date: 14 July 2015  
Revised date: 26 January 2016  
Accepted date: 28 February 2016

Please cite this article as: Minati Baral, Amit Gupta, B.K. Kanungo, Development of a  $C_3$ -symmetric benzohydroxamate tripod: Trimetallic complexation with Fe(III), Cr(III) and Al(III), (2016), doi: [10.1016/j.saa.2016.02.033](https://doi.org/10.1016/j.saa.2016.02.033)

This is a PDF file of an unedited manuscript that has been accepted for publication. As a service to our customers we are providing this early version of the manuscript. The manuscript will undergo copyediting, typesetting, and review of the resulting proof before it is published in its final form. Please note that during the production process errors may be discovered which could affect the content, and all legal disclaimers that apply to the journal pertain.



## Development of a C<sub>3</sub>-symmetric benzohydroxamate tripod: Trimetallic complexation with Fe(III), Cr(III) and Al(III)

Minati Baral<sup>1\*</sup>, Amit Gupta<sup>1</sup> and B.K. Kanungo<sup>2</sup>

<sup>1</sup>*Department of Chemistry, National Institute of Engineering and Technology Kurukshetra, Haryana-136119, India*

<sup>2</sup>*Department of Chemistry, Sant Longowal Institute of Engineering and Technology, Longowal, Punjab-148106, India*

*Email: minatibnitkr@gmail.com, Telephone: +91(1744)233544*

### Abstract

The design, synthesis and physicochemical characterization of a C<sub>3</sub>-symmetry Benzene-1,3,5 - tricarbonylhydroxamate tripod, noted here as BTHA, are described. The chelator was built from a benzene as an anchor, symmetrically extended by three hydroxamate as ligating moieties, each bearing O,O donor sites. A combination of absorption spectrophotometry, potentiometry and theoretical investigations are used to explore the complexation behavior of the ligand with some trivalent metal ions: Fe(III), Cr(III), and Al(III). Three protonation constants were calculated for the ligand in a pH range of 2-11 in a highly aqueous medium (9:1 H<sub>2</sub>O: DMSO). A high rigidity in the molecular structure restricts the formation of 1:1 (M/L) metal encapsulation but shows a high binding efficiency for a 3:1 metal ligand stoichiometry giving formation constant (in β unit) 28.73, 26.13 and 19.69 for [M<sub>3</sub>L]; M= Fe(III), Al(III) and Cr(III) respectively, and may be considered as an efficient Fe-carrier. The spectrophotometric study reveals of interesting electronic transitions occurred during the complexation. BTHA exhibits a peak at 238 nm in acidic pH and with the increase of pH, a new peak appeared at 270 nm. A substantial shifting in both of the peaks in presence of the metal ions implicates a s coordination between ligand and metal ions. Moreover, complexation of BTHA with iron shows three distinct colors, violet, reddish orange and yellow in different pH, enables the ligand to be considered for the use as colorimetric sensor.

Keywords: Spectrophotometric, potentiometric, hydroxamate, formation constants, protonation constants

## 1. Introduction

Hydroxamic acids,  $R_1C(O)N(R_2)OH$ , where  $R_1$ =alkyl/aryl and  $R_2$ = alkyl/aryl or H are ubiquitously known ligands in coordination chemistry for their high binding affinity for wide range of transition metal ions, and have received much attention in biological, analytical, chemical, medical and industrial field offering broad applications, particularly as clinical iron removing agents [1-3]. They form stable chelates with various metal ions attributing to their inhibitory action against enzymes having metalloprotein as their functional group [2-4]. The solutions of these organic molecules produce intense color complexes contributing widely in analytical chemistry as well as spectrophotometry for determination of metals [5-7]. Moreover, a significant adsorption of metals (mainly iron) by hydroxamate may play a beneficial role in recovery of metals from ground/waste water. Such as, excess metals dissolved in water caused toxic concentration as in acid mine drainage, posing multiple health problems such as high accumulation of iron in body, causing hemochromatosis [8]. Moreover, Al(III) a non-essential element, is involved in causing dialysis dementia in patients and affecting the central nervous system that causes different disorders such as amyotrophic lateral sclerosis [9-10]. The only approved drug, desferrioxamine B (iron chelator) for hemochromatosis is posing several drawbacks and side effects [11]. Although  $Cr^{+3}$  is absorbed by biological system, still, a high instance of occupational exposure to this trivalent metal pertained with respiratory problems like coughing, wheezing and dyspnea. Dermal exposure to chromium has also been demonstrated to produce irritant and allergic contact dermatitis [12]. Moreover, industrial effluents also have high concentration of dissolved chromium which causes chromium toxicity in nearby water resources. So, to deal with such situations, some molecules are under necessity to reduce overload of Fe(III), Cr(III) and Al(III) ions in an eco-friendly manner.

Despite of ongoing several researches for elucidating hydroxamate behavior, they remain poorly characterized. Possibilities of several conformations depending on concentration, temperature and the nature of the solvent attributes to the biggest challenge in hydroxamic acid characterization. A detailed comparative study is thus required to evaluate the capability of the ligand to serve as a potential chelator. High Stability constants of hydroxamic acids with transition metal ions can be considered as an important tool for elucidating chelating (polarizing) power of the ligands. The preferential binding mode in the metal hydroxamic acid complexes is

through O, O (bidentate) donors in which the ligand is either monobasic (hydroxamato) or dibasic (hydroximato) [13-15].

Hard metals with higher oxidation states preferentially form more stable hydroxamate complexes. Benzohydroxamic acid (Bha), acetohydroxamic acid (Aha), salicylhydroxamic acid and desferrioximine family (derived from *Streptomyces* species) are few hydroxamic acids dominating the coordination chemistry and chemical biology. The Bha is extensively used as an excellent spectrophotometric reagent for determination of metal ions such as Fe, Mo, V, U, and Mn, and could be served as a potential colorimetric reagent [16]. Synthesis and studies of a number of mono benzohydroxamates with various divalent and trivalent metal ions have been documented [17-18]. Trimesic acid coated alumina has been reported as a potent adsorbent for iron [8]. Considering the implications of Bha in analytical chemistry, there arises a burgeoning interest in increasing the substitution and exploring the coordination behavior in relation with the enhanced metal selectivity, efficiency and affectivity.

However, realizing the efficiency of hydroxamic acids as an efficient metal binder, it was thought for a higher substitution on benzohydroxamate which may offer an increased metal chelation in quantity, hence may be served as a potential metal scavenger. Keeping in view of the above, in the present communication we describe the development and complexation studies of a multidentate polyfunctional benzene-1,3,5-tricarbonylhydroxamic acid (BTHA). The potentiometric and spectrophotometric studies also explore the coordination behavior of the ligand with Fe, Al, and Cr trivalent metal ions in highly aqueous medium, H<sub>2</sub>O: DMSO = 9:1. Due to a rigid molecular framework and the coordination ability of three equally spaced hydroxamate groups, BTHA can serve as a strong metal-chelator and may find its use as a potent in applications in the areas such as acid mine drainage carrying excess dissolved iron at low pH.

## 2. Experimental

### 2.1 Materials and Measurements

Ultrapure grade reagents such as trimesic acid, methylchloroformate, N-methylmorpholine were purchased from Sigma Aldrich for the synthesis as well as titration purposes and used directly

without further purification unless otherwise mentioned. Analytical grade solvents: dimethylformamide, methanol, tetrahydrofuran and dimethylsulphoxide were purchased from Qualigens and SD Fine Chemicals Limited and distilled over appropriate drying agents as per standard procedures prior to use. Melting points were determined on MICROSIL digital melting point apparatus and were uncorrected.

The progress of the reaction and the purity were monitored by thin layer chromatography (TLC), performed on silica gel glass plates using 8:2 hexane and ethylacetate mixture and were visualized in iodine vapors. CHN elemental analyses were performed on Euro EA 3000, 60Hz-1200W elemental analyzer. UV spectrophotometric titrations were done on Thermofisher UV-VISIBLE spectrophotometer. The potentiometric and spectrophotometric studies were carried out in 9:1 :: H<sub>2</sub>O: DMSO mixture. The ionic strength was adjusted to 0.1 M KCl and the temperature was maintained at 25 ± 1 °C. The stock solutions were prepared in Millipore grade deionized water and for weighing the appropriate amount, high precision electronic balance CAS-CAUW220D was used that measures up to a level of four digits. KOH and HCl were standardized by acid-base titration method using 0.1M potassium hydrogen phthalate as primary standard and the exact concentrations were determined. 0.1M solutions were prepared freshly immediately before use in ultrapure deoxygenated water that was flushed in continuity with inert N<sub>2</sub> to remove CO<sub>2</sub> and O<sub>2</sub>.

The <sup>1</sup>H and <sup>13</sup>C NMR spectra of the ligand were obtained in d<sub>6</sub>DMSO using Bruker Avance II 400 NMR spectrometer. The chemical shifts were quantified in δ values (ppm). Tetramethylsilane (TMS) was used as an internal reference. The FT-IR spectra were obtained in the transmission mode as KBr pallet with Perkin- Elmer FT- IR spectrometer SPECTRUM 1000 in Mid-IR region range (4000- 400 cm<sup>-1</sup>).

## 2.2 Synthesis of Benzene-1,3,5- tricarbonylhydroxamic acid (BTHA)

In the synthesis of BTHA, the solvents used were freshly distilled and dried as per standard method [19]. The synthesis is illustrated below as scheme 1. A solution of 2.83 g of methylchloroformate (30.0 mmol) in 20 ml dimethylformamide was maintained at nearly -5°C using ice/CaCl<sub>2</sub> mixture and was stirred till a clear solution is obtained in step 1. 2.10 g (10.0

mmol) of trimesic acid dissolved in 10 ml of dimethylformamide was added to the above solution followed by the addition of 3.03g (30.0 mmol) N-methylmorpholine. The mixture was allowed to stir for 15 minutes. Precipitate of morpholine chloride was filtered out and the pale yellow colored filtrate was kept at  $\sim 4$  °C. In step 2, 2.1 g (30.0 mmol) hydroxylamine hydrochloride in methanol (15.0 ml) was added to the methanolic solution of KOH (15.0 ml). The mixture was stirred for 15 minute at 0 °C. White precipitate of KCl was removed by filtration and the filtrate containing free hydroxylamine was maintained at low temperature (0 °C). In step 3, cold solution of pale yellow colored filtrate of step 1 was added drop wise in hydroxylamine with continuous stirring for 60 minutes at room temperature. The solution was concentrated under vacuum to which 20 ml of distilled water was added and extracted with ethyl acetate followed by evaporation under vacuum. White-grey colored residue thus obtained was further washed with distilled water and re-crystallized in ethylacetate/methanol mixture giving a white residue (yield: 1.83g, 72%,); m.p.: 210-214 C; FT-IR (KBr pellet,  $\text{cm}^{-1}$ ): 3370, 3168, 3019, 1649, 1586, 1048, 910;  $^1\text{H}$  NMR (400mHz, DMSO- $\text{d}_6$ ,  $\delta$  ppm) 10.8-11.8 (s, 3H), 8.6-9.6 (s, 3H), 8.2-8.5 (m, 3H);  $^{13}\text{C}$  NMR (DMSO- $\text{d}_6$ ,  $\delta$  ppm): 166, 129, 127; and CHN analysis experimental (calculated) for  $\text{C}_9\text{H}_9\text{O}_6\text{N}_3$  found to be C = 42.12% (42.45%), N = 16.62% (16.54%), H = 3.41% (3.64%).

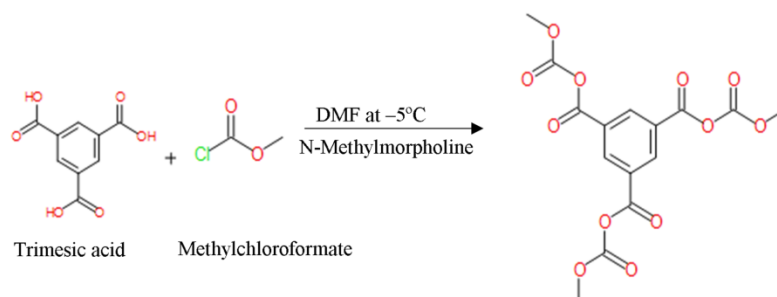
### 2.3 Potentiometric and spectrophotometric titration procedure

Potentiometric and spectrophotometric methods were employed to determine the ligand protonation constants and binding constants with the trivalent metal ions. Both the titrations were carried out in a double wall glass jacketed titration cell and the temperature was maintained at  $25 \pm 1$  °C by using a constant temperature circulating bath. The potentiometric titrations were done on HACH Sension-2 potentiometer using glass electrode that recorded pH as  $-\log[\text{H}^+]$ .

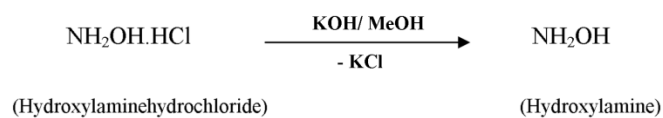
The electrode was duly calibrated in suitable buffers prepared by  $\text{H}_2\text{O}$ -DMSO 9:1 mixture following standard chemical method [19]. Borosilicate glass micro burette with least count 0.01ml was used for all titrations by using 9:1  $\text{H}_2\text{O}$ : DMSO mixture. The ligand solution (2 ml,  $1 \times 10^{-2}\text{M}$ ) was acidified with 2.0 ml of 0.1M HCl and titrated against standardized 0.1M KOH in 10% DMSO-water mixture at  $\mu = 0.1\text{M}$  KCl at  $25 \pm 1$  °C to determine the protonation constants in pH range 2.0 to 11.0. Complexation behavior of BTHA towards Fe(III), Cr(III) and Al(III) were studied by titrating 1:1 (2 ml,  $1 \times 10^{-2}\text{M}$  and 2 ml,  $1 \times 10^{-2}\text{M}$ ) and 3:1 (6 ml,  $1 \times 10^{-2}\text{M}$  and 2 ml,

$1 \times 10^{-2}$  M) metal-ligand mixtures against KOH, and formation constants ( $\log \beta$ ) of metal complexes were determined. Final concentration of ligand and metal were maintained as  $1 \times 10^{-3}$

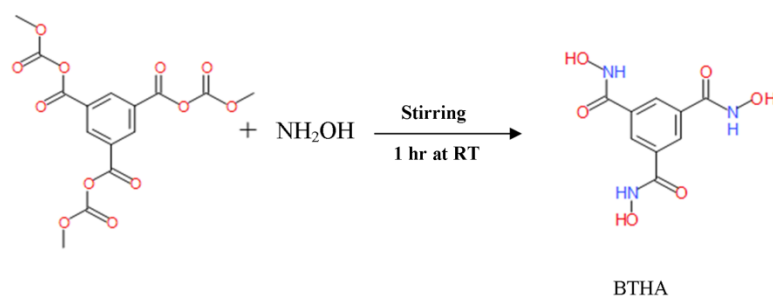
Step 1:



Step 2:



Step 3:



Scheme 1. Schematic representation of synthesis of tripodal ligand BTHA

and  $3 \times 10^{-3}$  M respectively for the titrations by keeping the total volume of 20 ml. The titration data was refined by the non-linear least square refinement program Hyperquad 2006 [20]. The formation of protonation and metal-ligand equilibria and their formation constants ( $\beta$ ) are defined in equation 1.



$$\beta_{pqr} = [\text{M}_p\text{H}_q\text{L}_r] / [\text{M}]^p[\text{H}]^q[\text{L}]^r$$

The species distribution curves at different pH were plotted with HYSS 2009 [21].

#### *2.4 Computational methods*

All calculations were carried out on a Pentium R (IV) 3.20 GHz machine in Window XP environment using HyperChem version 7.5 [22]. The initial geometry of BTHA molecule leading to minimum strain energy was achieved through molecular mechanics calculation using MM<sup>+</sup> force field. The periodical search to global minimum energy conformer of the ligand and its metal complexes were achieved using molecular dynamics simulation up to 2000 K followed by the MM<sup>+</sup> calculation. The minimum strain energy structures were further re-optimized through semi-empirical (PM3) self-consistent fields (SCF) method, at the Restricted Hartree-FOCK (RHF) level. The geometry optimizations were done by the application of the steepest descent method followed by the Polak-Ribere method with convergence limit of 0.0001 kcal/mol and RMS gradient of 0.001kcal/mol. For all the possible metal chelates, six coordinated structures were drawn by adding appropriate number of water molecules with the metal ions considering oxidation state of the metal ions. The electronic spectra of the various protonated and deprotonated species of the ligand were calculated through semi-empirical methods applying ZINDO/S Hamiltonian by using CAChe Work System Pro version 6.11 [23]. The full vibrational analysis was carried out for the ligand to obtain free energy in values by applying semi-empirical PM3 Hamiltonian. Prior to property calculations all the global minimum structures of the ligand and the coordinated compounds were checked for imaginary frequency.

### **3. Results and Discussion**

#### *3.1 Synthesis and characterization of ligand*

The polydentate chelator BTHA was obtained as white powder with a yield of 72% (pure) in three steps as given in scheme 1. The compound is completely soluble in DMSO, partially soluble in water and insoluble in methanol, ethanol, chloroform and tetrahydrofuran. It is stable to air and light. Structural characterization of the molecule was done by analyzing the chemical shifts ( $\delta$ ) in the <sup>1</sup>H and <sup>13</sup>C NMR spectra, FT-IR transmission data and CHN elemental analysis.

BTHA exists in two forms: E and Z amide form (Fig.1). Both of the isomers can be identified by characteristics infrared frequencies. The FT-IR spectrum of BTHA indicated several peaks

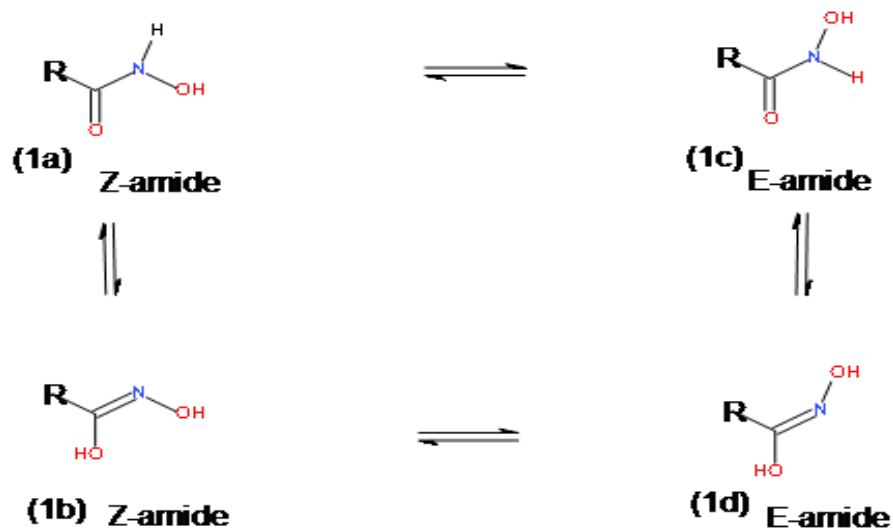


Fig. 1. Schematic representation of Z and E-amide isomers of hydroxamic acid

corresponding to various groups present in the molecular structure (Fig. 2) and the transmission values were analyzed and compared with the identified values in the literature [24]. The sharp band at  $3168\text{ cm}^{-1}$  corresponds to amide type  $\text{-NH}$  stretch while a broad band obtained at  $3370\text{ cm}^{-1}$  attributing for  $\text{-OH}$  stretch were obtained. The plausible explanation behind the prominent band at  $3019\text{ cm}^{-1}$  observed in the IR spectra is due to the Fermi-resonance overtone of CNH bend + C-N stretch. The transmission value at  $1640\text{ cm}^{-1}$  and  $1048\text{ cm}^{-1}$  indicated the presence of  $\text{-C=O}$  and  $\text{-N-O}$  group respectively in the substituted arms. The shifting in the transmission value of free  $\text{-OH}$  stretch from  $3600$  to  $3370\text{ cm}^{-1}$  and carbonyl group from  $1690$  to  $1640\text{ cm}^{-1}$  implicates intra-molecular H-bonding between  $\text{-OH}$  and nearly oriented carbonyl group, which is possible in the Z form of BTHA. Moreover, the appearance of the peak at  $1586\text{ cm}^{-1}$  also supports the predominance of Z isomeric form over E-form. As reported in the literature, CNH bend shows peak at  $1586\text{ cm}^{-1}$  corresponding to a characteristic peak for the Z isomer while the peak at  $1490\text{-}1440\text{ cm}^{-1}$  is characteristic for the E-isomer [24-25]. The vibrational spectrum obtained by semi empirical method using PM3 parameter showed closest agreement in terms of pattern of peaks with the experimental one and confirms the assignments. Predominance existence of Z-isomer of the ligand with a configuration of higher stability over E-isomer was

well supported, and, also helped in predicting the non-bonded interaction in the molecule. The approximate distance between the carbonyl oxygen and hydroxyl hydrogen in Z-amide form was found to be 2.682 Å clearly indicates the presence of intra molecular H-bonding [22], which is also evident in the experimental IR spectrum of the ligand.

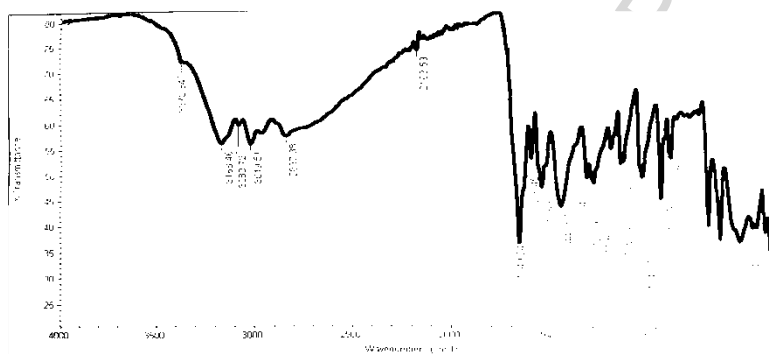
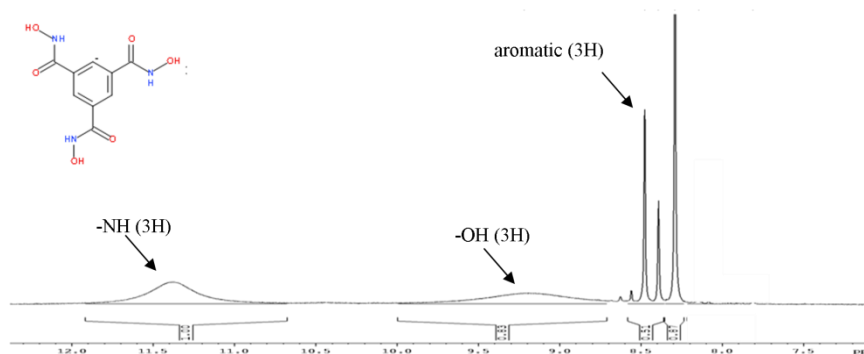


Fig. 2. FT-IR spectrum of BTHA

The  $^1\text{H}$  and  $^{13}\text{C}$  NMR spectra of the compound under investigation with their characteristic peaks are given in fig. 3. A singlet in the region 10.8 – 11.8 ppm attributes to the –NH group which may be due to quadrupole broadening as observed in case of nitrogen [26]. Another broad band appearing at ca. 8.6 – 9.6 ppm indicates presence of –OH group. A multiplet was obtained for aromatic hydrogens in the region 8.3 – 8.5 ppm. The  $^{13}\text{C}$  NMR spectrum illustrates the absorption signal for the carbonyl carbon at 163 ppm while for aromatic carbons gave chemical shift at 127 and 129 ppm.



**a**

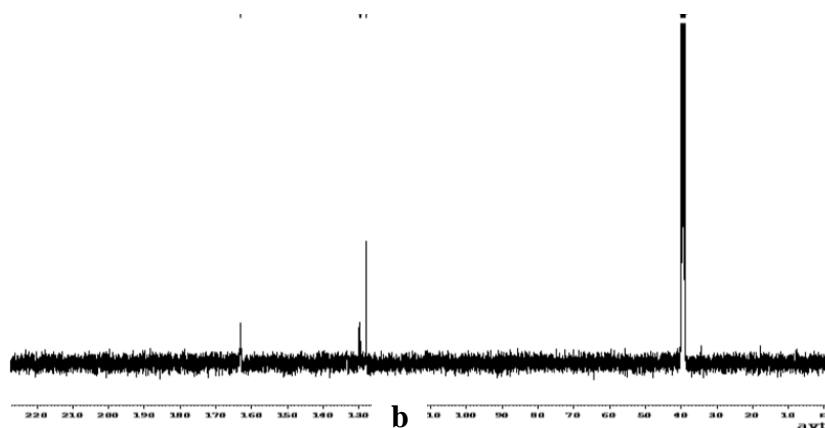


Fig. 3. (a)  $^1\text{H}$  NMR and (b)  $^{13}\text{C}$  spectra of BTHA in  $\text{DMSO-d}_6$  obtained on Bruker Avance II 400 NMR spectrometer

The ligand in 10% DMSO-water mixture shows only one peak at 238 nm which is due to  $\pi \longrightarrow \pi^*$  transition, associated with the aromatic ring [27]. The simulated electronic spectra obtained from semi-empirical/ZINDO/s method on PM3 optimized geometry also showed similarity in the peaks pattern as shown in fig. 4a. The pictorial representation of corresponding HOMO-LUMO molecular orbitals of the ligand causing transitions at aforesaid wavelength are given in fig. 4b.

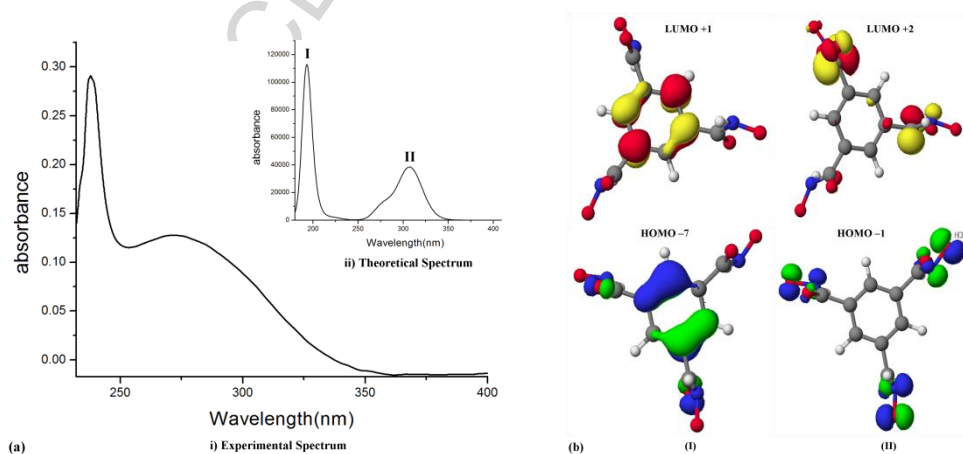


Fig. 4. (a) Electronic spectra of BTHA: (i) Experimental; (ii) Theoretical; (b) major transitions  $\text{HOMO-7} \rightarrow \text{LUMO+1}$  and  $\text{HOMO-1} \rightarrow \text{LUMO+2}$ , for two peaks at (I) and (II) respectively, calculated by Semi-empirical/ZINDO/s

### 3.2 Ligand protonation constants

The protonation constants of the ligand BTHA, which may be considered as triprotic  $LH_3$ , were determined by potentiometric and spectrophotometric methods. Due to the solubility problem of the ligand, the potentiometric titrations were carried out in 10% DMSO-water mixture, at  $\mu = 0.1$  M KCl and  $25 \pm 1$  °C. The potentiometric titration curves of pH versus 'a', where a= the moles of the base added per mole of the ligand, is presented in fig. 5. Inflection at a = 0 corresponds to neutralization of the excess acid added whereas the other inflection at a = 3 implied the consumption of base for the release of three moles of protons from the triprotic ligand. Analysis of potentiometric data gave three protonation constants as best fit calculated from Hyperquad using the equilibrium reactions as shown by the equation 2.

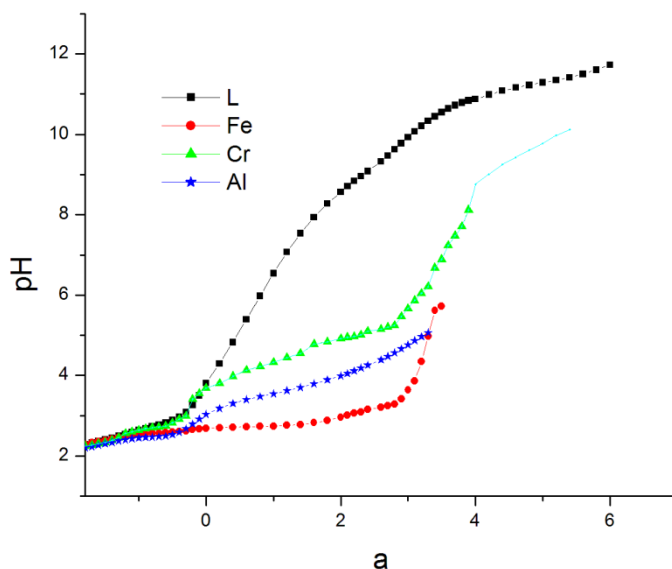
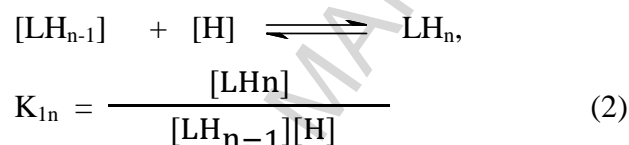


Fig.5. Potentiometric titration curves of the ligand between pH vs. 'a', in the absence and presence of the metal ions; M = Fe(III), Cr(III) and Al(III) in 3:1 metal-ligand ratio,  $[M] = 3 \times 10^{-3}$  M,  $[L] = 1 \times 10^{-3}$  M at  $\mu = 0.1$  M KCl and  $T = 25 \pm 1$  °C where 'a' = moles of base added per mole of the ligand

BTHA has six dissociable protons and behaves as hexaprotic acid. However, in the present study only three protonation constants for three –OH groups could be determined. Normally, N-acidity or O-acidity of hydroxamic acids depends upon the solvents used. In the presence of non-protic solvent (DMSO), hydroxamic acids favor N-acidity while aqueous polar solvent supports O-acidity [26]. Further, the amide protons require a high pH condition for the deprotonation due to poor acidity [28]. Hence, the three protonation constants due to the –NH groups could not be determined under the present experimental conditions. The simulated curve did not match with the experimental curve if the species  $LH_1$ ,  $LH_2$  and  $LH_3$  were considered only in the refinement process. Inclusion of the hydrolyzed species  $LH_{.1}$  and  $LH_{.3}$  gave the best fit. Further, above pH ~ 9, nature of curve indicated no steep change in pH value which could be explained due to the possibility of hydrolysis in the hydroxamic acids. The mechanism of hydrolysis reactions is cited in fig. 6.

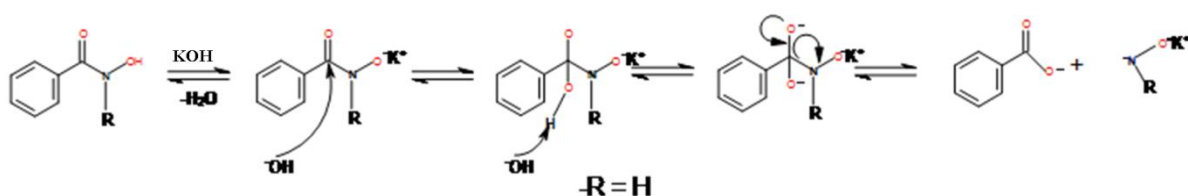


Fig. 6. Plausible mechanism of hydrolysis of BTHA in alkaline medium( shown only at one arm)

The hydrolysis of hydroxamic acids in the basic medium is well-documented [29]. The mechanism accounted for the hydrolysis of BTHA at higher pH, involves attack of  $OH^-$  ion at the carbonyl group in the presence of polar aqueous solvent forming salt of carboxylic acid and hydroxyl amine eventually. The different species of the chelator formed are  $LH_1$ ,  $LH_2$ ,  $LH_3$ ,  $LH_{.1}$ ,  $LH_{.3}$  in the adopted pH range. The species distribution curve is given in fig. 7 (a).  $LH_3$ , the fully protonated form, initially exists in 100% (at  $pH < 5.0$ ). As the pH increases, deprotonation starts with the formation of  $LH_2$  and  $LH$  species with the maximum formation of 70 % and 60 % at pH 7.8 and 9.0, respectively. For further confirmation of the species formed and the corresponding protonation constants obtained by the potentiometric method, spectrophotometric titrations were carried out in a highly aqueous-DMSO mixture (9:1) at  $1 \times 10^{-5}$  M ligand concentration,  $25 \pm 1^\circ C$  and constant ionic strength 0.1 M KCl. The measurements included absorbance with respect to pH of the solution. The electronic spectra of the ligand were recorded from 200-550 nm in a

wide pH range of 2.0-11.0 and are given in fig. 7(b). Protonation constants (log K) as well as hydrolysis constants of the ligand were obtained by the analysis of the experimental data from best fit curve using HypSpec simulating software [30] as depicted in table 1.

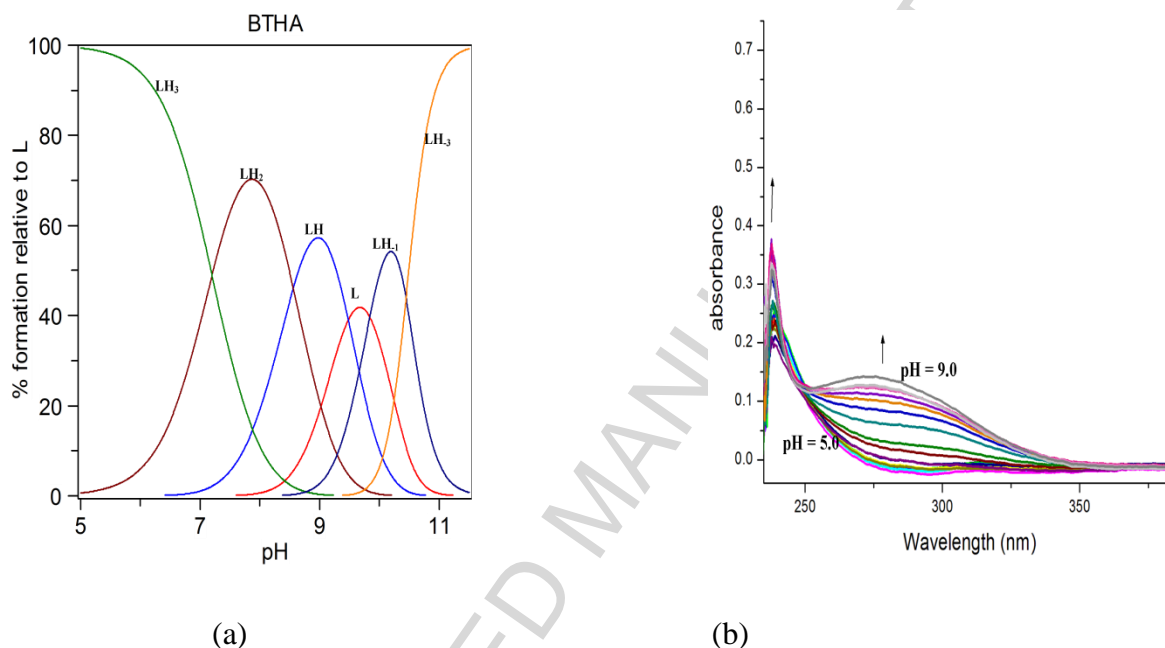


Fig. 7 (a). pH dependent distribution of the species of BTHA (b) Electronic spectra of BTHA as a function of pH (2.0 -11.0) during a spectrophotometric titration where  $[BTHA] = 1 \times 10^{-5}$  M, at  $\mu = 0.1$  M KCl and  $25 \pm 1^\circ\text{C}$

Table 1: Protonation constants (log K) and hydrolysis constants of BTHA at  $25 \pm 1^\circ\text{C}$ ,  $[L] = 0.1 \text{ mol dm}^{-3}$  and  $\mu = 0.1$  M KCl in  $\text{H}_2\text{O} / \text{DMSO} (9:1)$  in pH 2-11 obtained by potentiometric and spectrophotometric methods

Species	Potentiometry	Spectrophotometry
$[\text{LH}]/[\text{L}][\text{H}]$	$9.48 \pm 0.04$	$9.67 \pm 0.05$
$[\text{LH}_2]/[\text{L}][\text{H}]^2$	$8.56 \pm 0.03$	$8.74 \pm 0.03$
$[\text{LH}_3]/[\text{L}][\text{H}]^3$	$7.2 \pm 0.05$	$7.4 \pm 0.05$
$[\text{LH}_{-1}][\text{H}]/[\text{L}]$	$-9.84 \pm 0.02$	$-9.97 \pm 0.02$
$[\text{LH}_{-3}][\text{H}]^3/[\text{LH}_{-1}]$	$-21.89 \pm 0.04$	$-22.12 \pm 0.04$

No noticeable changes in electronic spectra were observed below pH 5.0 and above pH 9.0. The equilibrium states between protonated and non-protonated forms of the ligand were studied by examining the shifts in the ligands' peaks. The protonation constants obtained by

spectrophotometric method are in agreement with the results obtained by potentiometric method. The characteristic electronic absorbance spectra of benzohydroxamic acid similar mono substituted ligand have been reported [27].

Protonation constants of hydroxamic acids,  $R_1C(O)N(R_2)OH$  ( $R_1 = \text{alkyl/aryl}$ ,  $R_2 = \text{alkyl/aryl/H}$ ) depend upon the nature of  $R_1$  and  $R_2$ . The protonation behavior of some mono hydroxamic acids have been studied both in aqueous and solvent mixture media [31]. Acetohydroxamic acid (Aha) has higher protonation constant value due to the presence of electron donating group i.e.,  $R_1 = -CH_3$  when compared to Bha, where  $R_1 = -C_6H_5$  causes  $-I$  effect. Similarly in case of BTHA, substituted aromatic ring also influences the protonation constants ( $\log K$ ) as shown in table 2.

Table 2: Protonation constants ( $\log K$ ) of mono hydroxamic acids and tri-hydroxamic acids, BTHA in aqueous medium;  $T = 25^\circ C$ ,  $I = 0.2 \text{ mol/dm}^3 \text{ KCl}$  at  $\mu = 0.1 \text{ mol/dm}^3 \text{ KCl}$ ,  $25 \pm 1^\circ C$

Ligand	Aha	Pha	Hha	Bha	PhAha	MAha	iPAha	BTHA
$R_1$	$-CH_3$	$-C_2H_5$	$-(CH_2)_4CH_3$	$-C_6H_5$	$-CH_3$	$-CH_3$	$-CH_3$	
$R_2$	H	H	H	H	$-C_6H_5$	$-CH_3$	$-CH(CH_3)_2$	
$\log K$	9.27	9.33	9.36	8.69	8.47	8.70	9.26	9.36
	10.57*			9.93*				8.54
								7.24

\* in 50-50% (m/m)  $H_2O$ : DMSO

Literature studies reveal that benzohydroxamic acid has maximum absorbance at 228 nm in acidic and neutral pH. However, in alkaline condition it shows a new peak at 264 nm in addition to the earlier one due to stabilization of the excited state by charge delocalization which corroborates well of the existence of various forms in the basic medium as depicted in fig 8. The tautomer II fetches the stability through charge delocalization that brings the higher excited state  $\pi^*$  closer to the ground  $\pi$  state and reduces energy of the transition state. Similar pattern was also observed in the tri-hydroxamic acid substituted benzene (BTHA), a peak was observed at 238 nm in acidic medium and an additional broad peak appeared in the alkaline medium with  $\lambda_{max}$  at 270nm. Deprotonation of the fully protonated ligand  $LH_3$  causes formation of a new peak with concomitant rise in absorbance intensity due to the formation of  $LH_2^{-1}$ ,  $LH^{-2}$  and  $L^{-3}$  species. The

appearance of two peaks in the electronic spectra of the ligand justified by  $\pi \rightarrow \pi^*$  transitions of two tautomeric forms of BTHA existing in equilibrium [27].

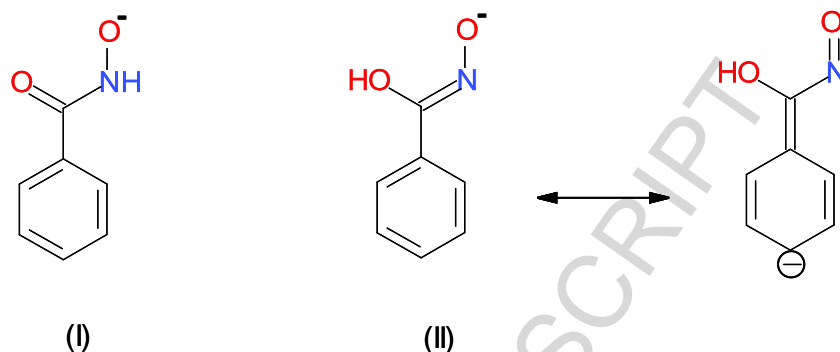


Fig. 8. Tautomeric forms of mono-substituted benzene hydroxamic acid (Bha)

### 3.3 Metal complex formation:

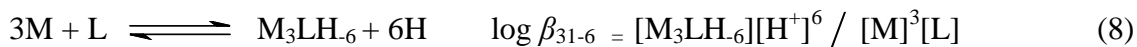
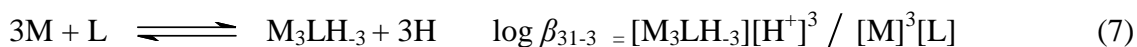
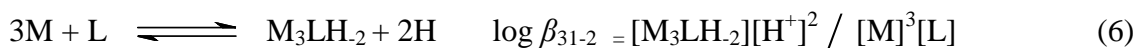
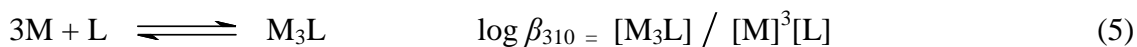
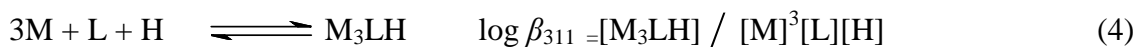
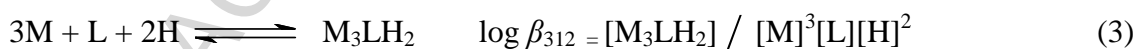
Complexation studies of BTHA with Fe, Cr and Al trivalent metal ions were conducted by potentiometric and spectrophotometric methods in 1:1 and 3:1 metal-ligand molar ratios at ionic strength  $\mu = 0.1\text{M}$  KCl and temperature  $25 \pm 1^\circ\text{C}$ . The titration curves of all the metal ions with the ligand in 3:1 ratio are shown in fig. 5. The symbols represent data collected when no turbidity or solid phase was there, whereas dashed lines represent points collected when solution becomes turbid. The precipitation occurred for Fe(III) and Al(III) in the pH range of  $\square$  5.3-6.0, whereas in case of Cr (III), no precipitation was occurred. The volume of base used up to 'a' = 3, indicates the release of three moles of protons from BTHA upon complexation with the metal ions. The buffer region of the ligand shifted towards lower pH in the presence of metal ions with the release of dissociable protons from the ligand. The larger deviation in the Fe-L curve from the ligand only curve was more towards lower pH relative to the Cr-L and Al-L, indicates strong complex formation between iron and the ligand. Hyperquad 2006 program was used for calculating formation constants of the species using  $\log \beta$  values of the ligand as input data. The results are summarized in table 3. The best fit model obtained after simulation substantiated the presence of  $\text{M}_3\text{LH}_2$ ,  $\text{M}_3\text{L}$  species for Fe(III) and Al(III) metal ions, while  $\text{M}_3\text{LH}$  and  $\text{M}_3\text{L}$  species were formed in case of Cr(III) metal ions.

It has been well-established that metal ions exist as hexacoordinated  $[\text{M}(\text{H}_2\text{O})_6]$  in aqueous solution [32]. BTHA occupies two coordination sites of each metal ion through O, O- donor

atoms, while rest sites were occupied by four water molecules. In the presence of Fe (III) and Table 3: The overall formation constants ( $\log \beta$ ) of the metal complexes at  $25 \pm 1^\circ \text{C}$  and  $\mu = 0.1 \text{ M KCl}$  (A= Potentiometry and B = Spectrophotometry)

	Fe(III)		Cr(III)		Al(III)	
	A	B	A	B	A	B
$[\text{M}_3\text{LH}_2]/[\text{M}]^3[\text{L}][\text{H}]^2$	$34.35 \pm 0.03$	$34.08 \pm 0.08$	-----	-----	$33.98 \pm 0.03$	$34.29 \pm 0.08$
$[\text{M}_3\text{LH}_1]/[\text{M}]^3[\text{L}][\text{H}]$	-----	-----	$23.55 \pm 0.09$	$23.81 \pm 0.09$	-----	-----
$[\text{M}_3\text{L}]/[\text{M}]^3[\text{L}]$	$28.73 \pm 0.07$	$28.98 \pm 0.03$	$19.69 \pm 0.08$	$19.83 \pm 0.05$	$26.13 \pm 0.08$	$26.19 \pm 0.06$
$[\text{M}_3\text{LH}_2][\text{H}^+]^2/[\text{M}]^3[\text{L}]$	$21.69 \pm 0.03$	$21.89 \pm 0.08$	$8.28 \pm 0.04$	$8.36 \pm 0.04$	$16.52 \pm 0.03$	$16.84 \pm 0.04$
$[\text{M}_3\text{LH}_3][\text{H}^+]^3/[\text{M}]^3[\text{L}]$	$16.54 \pm 0.05$	$16.87 \pm 0.04$	$2.40 \pm 0.03$	$2.86 \pm 0.04$	-----	-----
$[\text{M}_3\text{LH}_6][\text{H}^+]^6/[\text{M}]^3[\text{L}]$	$-1.22 \pm 0.03$	$-1.45 \pm 0.04$	$-19.76 \pm 0.03$	$19.89 \pm 0.04$	$-4.15 \pm 0.05$	$-4.65 \pm 0.03$

Al(III) ions, precipitation occurred between pH 5.3-6.0, either due to hydrolysis of metal ions or by the formation of mixed metal-ligand hydrolyzed species. No precipitation was observed in case of Cr (III) till pH 11.0. Data above pH  $\sim 8.5$  was not included in the calculation due to the hydrolysis of the ligand as discussed earlier. Inclusion of hydrolyzed species  $\text{M}_3\text{LH}_2$ ,  $\text{M}_3\text{LH}_3$ ,  $\text{MLH}_6$  for Fe(III) and Cr(III); and  $\text{M}_3\text{LH}_2$ ,  $\text{M}_3\text{LH}_6$  for Al(III) in the model, gave complete match of the theoretical and experimental curves. Possibility of formation of 1:1 ML encapsulated complex or mono/dimetallic-complex were discarded as their inclusion in data either worsen the refinement process or did not bring any improvement in the curves. Various species can be represented by the following equilibria:



In order to explore the nature of the precipitates obtained during the titrations of Fe (III) and Al(III), the precipitates were filtered, washed with distilled water, dried and analyzed through IR spectroscopic studies (Fig.9). The IR spectra of the precipitates were found to contain peaks of of BTHA with a negative shift of  $\sim 24\text{-}37\text{ cm}^{-1}$  corresponding to  $\nu\text{C}=\text{O}$ , might be due to the shifting of charge density due to complex formation with the metal ions. This confirms, the precipitates obtained during experiment above pH 5.3 are due to the M-L complexes, and the ligand coordinates to the metal ions through two oxygen atoms of each hydroxamate arm.

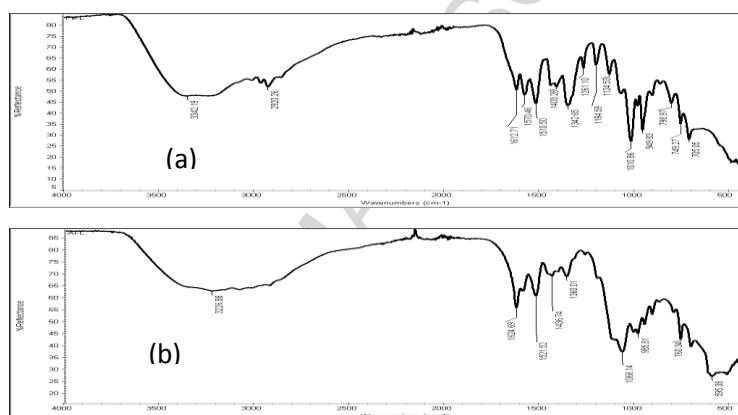


Fig. 9. IR spectra of precipitates obtained for: a) Fe-BTHA; b) Al-BTHA

Alston *et al.*, also claimed the formation of five membered ring complex through O, O-coordination exhibiting violet color at low pH (Fig. 10) [33].

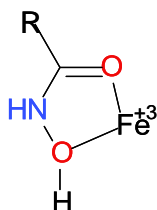


Fig. 10. Coordination of iron with hydroxamate at low pH forms five member ring

The species distribution curves (Fig. 11) show that in an acidic medium (pH  $\sim 2.0$ ) ligand forms protonated metal complex  $\text{M}_3\text{LH}_2$  with 80 % formation for both Fe and Al metal ions but, no

such protonated species exists except  $M_3LH$ , for the Cr ion with 17% formation only. With the increase in pH, deprotonation of  $M_3LH_2$  led to the formation of trimetallic  $M_3L$  species with maximum formation of 85% at pH  $\sim 3.0$  and 78 % at pH $\sim 4.2$  for Fe(III) and Al(III) metal ions respectively. For Cr (III),  $M_3L$  species was formed with 60% at pH  $\sim 5.2$ .

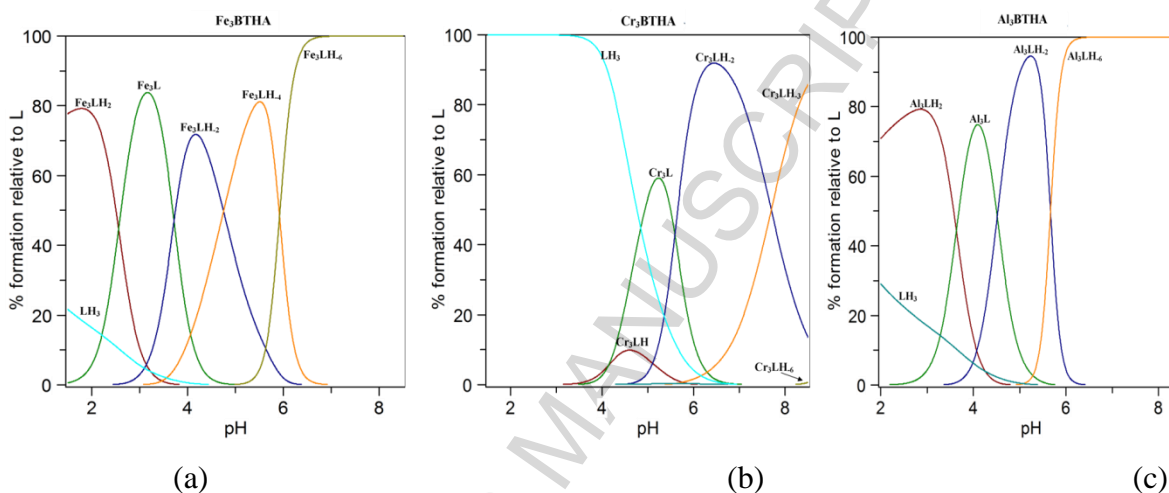


Fig. 11. pH-dependent distribution curves of the species of BTHA metal complexes (a) Fe(III), (b) Cr(III) and (c) Al(III)

The interaction of transition metal ions with the ligand BTHA, was also studied by UV-Visible spectrophotometric method in 3:1 metal-ligand stoichiometry ratio. The concentrations of the ligand,  $[L] = 1.0 \times 10^{-5}$  M, and metal ion,  $[M] = 3 \times 10^{-5}$  M were used to study the complexation behavior in the wavelength range of 200-550 nm with the increasing of pH to elaborate different possible forms of the species formed in the solution. The ligand metal interaction accompanied with major spectral changes, has been depicted in fig. 12.

The hyperchromic shift in the ligand peaks in the presence of the metal ions implied the coordination of the chromophoric group of the ligand with the metal ions. In case of Fe-BTHA, the intensities of both the bands were higher as compared to the bands of BTHA, whereas, in case of Cr(III)-BTHA and Al(III)-BTHA the intensities were lower. Complex formation between BTHA and Fe(III) ion at pH  $\sim 2$ , was further evidenced by the appearance of a dark violet coloration during the titration. The broad band at 430 nm is attributed to  $L \rightarrow M$  charge transfer transition.

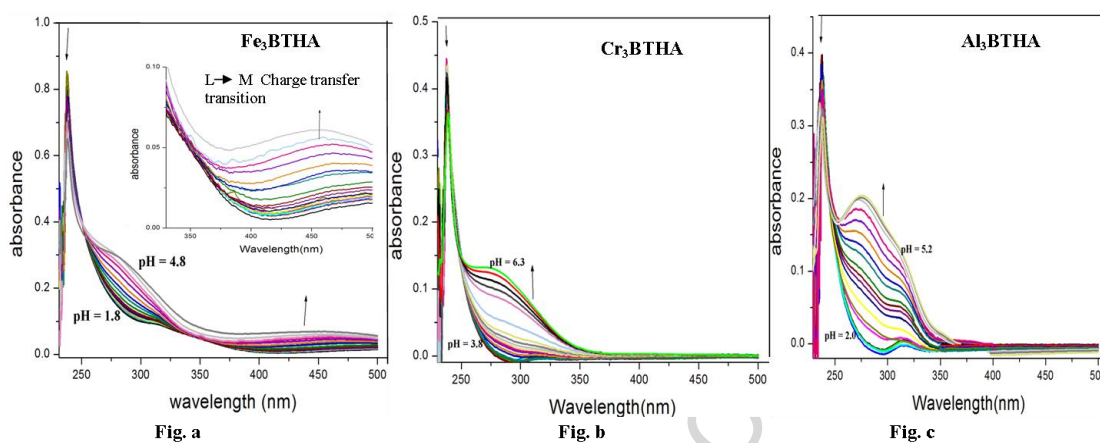


Fig. 12. Electronic spectra of BTHA as a function of pH (2-11) during spectrophotometric titration with (a) Fe(III), (b) Cr(III) and (c) Al(III),  $[M]=3\times 10^{-5}M$ ,  $[L]=1\times 10^{-5}M$  in H<sub>2</sub>O/DMSO (9:1) mixture at  $\mu = 0.1 M$  KCl at  $T=25 \pm 1^\circ C$

Above pH 2.5, a reddish orange color along with a hyperchromic effect in the absorption spectra was observed which may be due to the formation of  $M_3L$  species, as evident from the species distribution curve. Further increase in pH ( $> 5.0$ ) caused formation of a yellow color. The significant color variation in case of Fe-BTHA complex in a largely aqueous medium is due to the allowance of a ligand to metal charge transfer transition involving protonated and deprotonated species formed at varied pH. Fig. 13 represents distinct colour variations in BTHA-Fe as a function of pH. Although complexation of the ligand with Cr(III) and Al(III) occurred, no coloration was observed due to a negligible or no charge transfer transition.

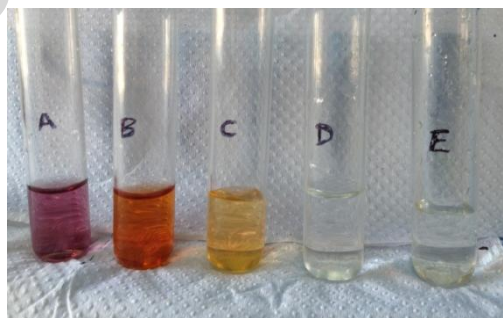


Fig. 13. BTHA metal complexes in H<sub>2</sub>O/DMSO (9:1) solution exhibits color at different pH. Fe-BTHA complex in test tube A: violet, pH 1.8-2.5; B: reddish orange, pH 2.5-5.0, C: yellow, pH  $> 5.0$ ; D and E represent Cr-BTHA and Al-BTHA complex respectively showing no noticeable color

The complexation ability of a ligand towards a metal ion at particular pH is better represented by pM values. Metal ions compete with the protons during complexation in the solution, which mainly depends upon pH and pK<sub>a</sub> of the ligand. The corresponding plots of pFe, pAl and pCr versus pH over a range of 2-9, [L] = 10<sup>-3</sup>M and [M] = 3×10<sup>-3</sup>M were shown in fig.14. The pM value for Fe<sup>+3</sup> (5.25) at pH 5.5 is relatively high as compared to Al<sup>+3</sup> and Cr<sup>+3</sup> (4.5 and 3.5) indicating maximum complexation of BTHA with iron followed by Al and then Cr trivalent ions. The strong coordination ability of the trisubstituted hydroxamate tripod, BTHA, in acidic pH and subsequent precipitation formation of the complexes near pH 5.5 enables it to be considered as effective sequestering agent for both Fe<sup>+3</sup> and Al<sup>+3</sup> ions.

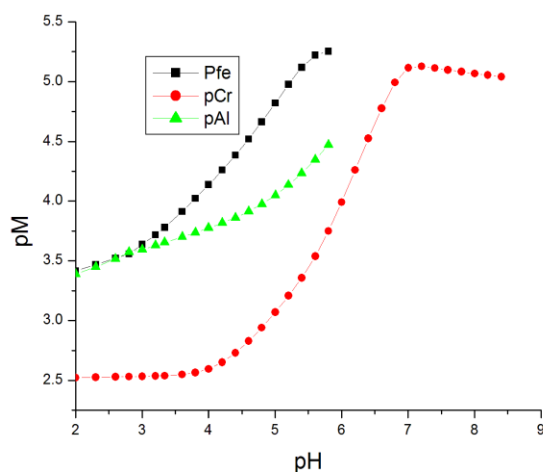


Fig. 14. Plot of pM versus pH for BTHA,  $pM = -\log[M]$ , calculated for  $[M^{+3}] = 3 \times 10^{-3}M$  and  $[L] = 1 \times 10^{-3}M$

To verify the validity and agreement of the stability constants determined, the thermodynamic properties of the species involved in the chemical equilibria were calculated by semi-empirical/PM3 method. Change in the free energy for the metal complexes  $[L(M(H_2O)_4)_3]$  where M=Fe(III), Cr(III) and Al(III) were evaluated as -5434.58, -4564.29, and -4859.75 kJ/mol respectively. The stability order:  $Fe^{3+} > Al^{3+} > Cr^{3+}$ , corroborates well with the experimental studies carried out by potentiometric and spectrophotometric methods and change in free energy of formation of metal complexes. The enhancement in the stability of Fe(III)-BTHA as compared

to chromium can be justified on the basis of Irving William stability order for transition metals [34], according to which the stability of some trivalent transition metal ions, given below, maintain the trend  $\text{Co}^{+3}(\text{low spin}) > \text{Mn}^{+3} > \text{Fe}^{+3} > \text{Cr}^{+3}$  irrespective of particular ligand involved. The trend observed by Irving William is largely determined by electrostatic effects and can be related to the ionic potential ( $Z/r$ ;  $Z$ = ionic charge and  $r$ = radius) as well as ionization potential (i.e.  $\text{M} \rightarrow \text{M}^{+n}$ ) of metal ions.

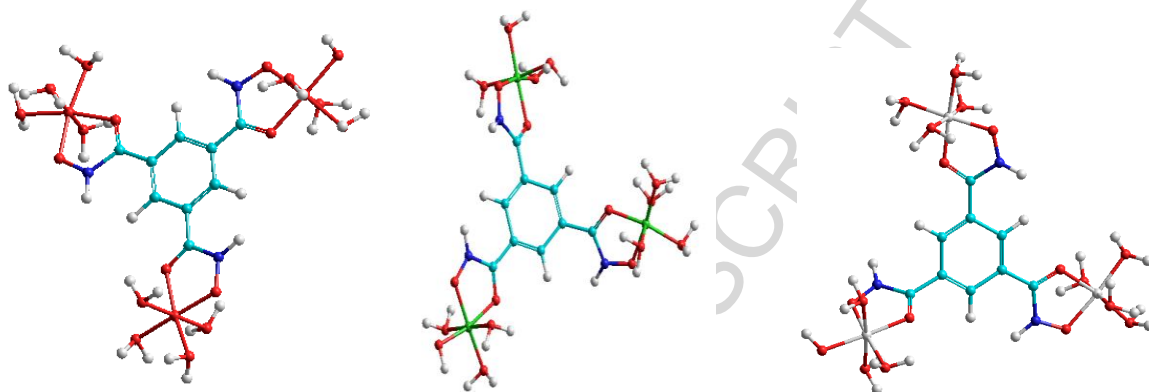
**Conclusions:** The newly synthesized tripodal polydentate ligand BTHA, with the arms of three hydroxamate binding moieties, shows greater binding efficiency towards Fe(III) as compared to Cr(III) and Al(III). High formation constants of 3:1 metal-ligand complexes,  $\text{M}_3\text{L}$ , can be explained due to coordination of three pairs of O, O donors in the ligand that show higher binding affinity towards hard metals, besides forming stable five membered rings chelates. As seen from the  $\log \beta$  values, the ligand BTHA was found to be excellent chelator towards Fe(III) in acidic range and may be beneficial in developing of a more efficient adsorbent for Fe(III) metal ions than the existing ones. Thus, the current ligand has the future prospect in reducing the effect of water pollution containing iron in toxic concentration. The tripod exists predominantly in Z-amide form which is favorable for intramolecular H-bonding. In the alkaline pH, BTHA deprotonates giving rises to tautomers which are evident by the appearance of a new additional peak in the electronic spectra of the ligand. Moreover, Fe-BTHA complex shows distinct colour variation (violet-reddish orange-yellow) at different pH due to  $\text{L} \rightarrow \text{M}$  charge transfer; this enlightens its role as effective colorimetric agent and as potential iron sensor.

## References

- [1] P. V. Bernhardt, Dalton Trans (2007) 3214-3220
- [2] R. Codd, Coord. Chem. Rev 252 (2008) 1387-1408
- [3] C. J. Marmion, D. Griffith, K.B. Nolan, Eur. J. Inorg. Chem 2004 (2004) 3003-3016.
- [4] I. M. Adcock, Curr. Med. Chem 7 (2006) 966-973
- [5] B. Kurzak, H. Kozlowski, E. Farkas, Coord. Chem. Rev 114 (1992) 169-200
- [6] Y. K. Agrawal and R. D. Roshania, Bull. Sot. Chim Belg 89 (1980) 159
- [7] S. G. Tandon and S. C. Bhattacharya, J Indian Chem. Soc No 47 (1970) 583
- [8] B. Saha, S. Chakraborty, G Das, J. Colloid Interface Sci 323 (2008) 26-32
- [9] M. Kawahara, M. Kato-Negishi, Int. J. Alzheimers Dis 2011 (2011) 276393
- [10] C. A. Shaw, M. S. Petrik, J. Inorg. Biochem 103 (2009) 1555
- [11] S. Simon, P. A. Athanasiov, R. Jain, G. Raymond, J. S. Gilhotra, Indian J. Ophthalmol 60 (2012) 315-317

- [12] a) L. Polak, In: D. Burrows (Eds) Chromium: metabolism and toxicity, FL: CRC Press,: 51-135  
b) H.S. Novey, M. Habib et al., J. Allergy Clin. Immunol 72 (1983) 407- 412.
- [13] R. Kakkar, R. Grover, P. Chadha, Org. Biomol Chem 1 (2003) 2200.
- [14] T. W. Failes and T.W. Hambley, Dalton Trans (2006) 1995-1901
- [15] C. J. Marmion, D. Griffith and K.B. Nolan, Eur. J. Inorg. Chem (2004) 3003-3016
- [16] R. Arora, R. Kakkar, Int. Rev. Biophys. Chem (IREBIC) 3 (2012) 212-233
- [17] M.M. Khalil and A.E.Fazary, Monatshefte fur Chemie 135 (2004) 1455-1474
- [18] E. Farkas and O.Szabo, Inorg. Chim. Acta 392 (2012) 354-361
- [19] B. S. Furniss, A. J. Hannaford, P.W.G. Smith, A.R. Tatchell, Vogel'S Textbook of Practical Organic Chemistry, Prentice Hall, 5<sup>th</sup> Ed, 2008
- [20] P. Gan, A. Sabatini, A. Vacca, Talanta,53 (1996) 1739
- [21] a) L. Alderighia, P. Gans, A.Ineco, D. peters, A. Sabatini, A. Vacca, Coord. Chem. Rev 184 (1999) 311
- [22] HyperChem Version 7.5, Hypercube Inc., 419 Phillip Street, Waterloo, Ontario, Canada, N2L, 3X2
- [23] CAChe version 6.11 (2003) Fujitsu Limited
- [24] a) F. S. Higgins, L. G. Magliocco, N. B. Colthup, Appl. Spectrosc. 60 (2008) 279-287  
b) A. Kaczor, J. Szczepanski, M. Vala, H. Kozlowski, L. M. Preoniewicz, Phys. Chem. Chem. Phys 5 (2003) 2337- 2343
- [25] B. Garcia, S. Ibeas, J.M. Leal, F. Secco, M. Venturini, M.L. Senent, A. Nino, C. Munoz, Inorg. Chem 44 (2005) 2908-2919
- [26] J. Schraml, M. Tkadlecova, S. Pataridis, L. Soukupova, V. Blechta, J. Roithova, O. Exner, Magn. Reson. Chem 43 (2005) 535-542
- [27] R. E. Plapinger, J. Org. Chem 24 (1959) 802-804
- [28] B.K. Kanungo, M. Baral, S.K. Sahoo, S.E. Muthu Spectrochimica Acta A: Molecular and Biomolecular Spectroscopy 74 (2009) 544-552.
- [29] a) A. Ahmad, J. Socha and M. Večeřa Collect. Czech. Chem. Commun 39 (1974) 3293-3303  
b) K. K. Gosh, K. K. Krishnani, S. Ghosh, Indian J. Chem 38B (1999) 337-342
- [30] P. Gans, A. Sabatini, A. Vacca, Ann. Chim. (Rome) 89 (1999) 45
- [31] E. Farkas, E. Kozma, M. Petho, K. M. Herlihy, Micera G, Polyhedron 17 (1998) 3331-3342
- [32] S. K. Sahoo, R.K. Bera, M. Baral, B. K. Kanungo, J. Photochem. Photobiol., A 188 (2007) 298-310.
- [33] W. C. Alston II, K. Ng, Forensic Sci. Int. 126 (2003), 114-117
- [34] A. Ciferri, and A. Perico, Ionic interactions in natural and synthetic macromolecules, John-Wiley & Sons, 2012

## Graphical Abstract



## Highlights

- A tri substituted hydroxamate tripodal ligand developed, forms thermodynamically stable complexes with high  $\log \beta$  and  $pM$  values with trivalent metal ions : Fe, Cr and Al.
- The ligand with short arms of hydroxamic acid renders restriction for a 1:1 ligand- metal encapsulation showing a large molecular strain energy
- Preferentially the ligand forms trimetallic complex of the type,  $[L(M(H_2O)_4)_3]$ , hence, can be applied as potent adsorbent of the metal ions in solution present in toxic concentration.
- Fe(III)-L exhibits three distinct colors (violet-reddish orange-yellow) at different pH implying the significant role of the chelator for the application as colorimetric sensor.
- The theoretical investigations confirm the experimental findings.